European Review for Medical and Pharmacological Sciences 2020; 24: 3805-3817

LncRNA SNHG7 enhances chemoresistance in neuroblastoma through cisplatin-induced autophagy by regulating miR-329-3p/MYO10 axis

S.-Y. WANG, X. WANG, C.-Y. ZHANG

Department of Pediatrics, The Fifth Affiliated Hospital of Harbin Medical University, Daqing City, Heilongjiang Province, China

Shuyue Wang and *Xue Wang* contributed equally to this work

Abstract. – OBJECTIVE: Neuroblastoma (NB) is a type of extracranial solid tumor that usually occurs in children. Drug resistance has become a major obstacle in NB chemotherapy. Long non-coding RNA small nucleolar RNA host gene 7 (SNHG7) is an oncogene in many cancers, including NB. This study aimed to investigate the role of SNHG7 in cisplatin sensitivity of NB and the underlying mechanism.

PATIENTS AND METHODS: Cell Counting Kit-8 (CCK-8) assay was used to detect cell viability, and the IC50 of cisplatin was calculated. The protein levels of autophagy markers were measured by Western blot assay. The levels of SNHG7, miR-329-3p and myosin X (MYO10) were examined by quantitative real-time polymerase chain reaction (qRT-PCR) or Western blot assay. The interaction among SNHG7, miR-329-3p and MYO10 was confirmed by Dual-Luciferase reporter assay.

RESULTS: Cisplatin curbed the viability of NB cells in a dose-dependent manner and facilitated autophagy in NB cells. Silencing of SNHG7 reduced cisplatin resistance and suppressed cisplatin-induced autophagy. SNHG7 was a sponge of miR-329-3p and modulated chemosensitivity and autophagy by regulating miR-329-3p. In addition, SNHG7 upregulated MYO10 by sponging miR-329-3p. MYO10 restored the effect of miR-329-3p on cisplatin sensitivity and autophagy. Moreover, suppression of autophagy blocked SNHG7-induced cisplatin resistance.

CONCLUSIONS: Depletion of SNHG7 potentiated cisplatin sensitivity through inhibition of autophagy by modulating miR-329-3p/MYO10 axis, providing a new therapeutic approach to overcome cisplatin resistance in NB chemotherapy.

Key Words:
SNHG7, MiR-329-3p, MYO10, Cisplatin, Autophagy, Neuroblastoma.

Introduction

Neuroblastoma (NB), a common extracranial solid tumor in children, is derived from neural crest cells of the sympathetic nervous system[1]. NB accounts for 15% of childhood cancer-related mortality[2]. According to different stages of NB, targeted treatments were adopted, including surgery, chemotherapy and radiotherapy[3]. Chemotherapy drugs commonly used in NB include cisplatin, cyclophosphamide and vincristine[4]. However, chemotherapy resistance has become a major obstacle to NB therapy[5]. Therefore, studying the molecular mechanisms of chemical resistance is critical to preventing drug resistance and improving the treatment of NB.

Autophagy is the process by which autophagosomes self-eat cells[6]. The hallmark of autophagy is the degradation of cellular components that are harmful or dysfunctional[7]. Autophagy exerts a crucial regulatory role in human diseases, especially inflammatory diseases, neurodegenerative diseases and cancer[8]. Microtubule-associated protein 1 light chain 3B (LC3B), p62 and Beclin-1 are considered to be markers of autophagy[9]. Emerging researches have elucidated that autophagy is related to the sensitivity of chemotherapy drugs[10].

Long non-coding RNAs (lncRNAs) are a class of non-coding RNAs longer than 200 nucleotides. LncRNAs are aberrantly expressed in many cancers and participate in tumorigenesis and development[11]. LncRNA small nucleolar RNA host gene 7 (SNHG7) has been verified to expedite tumor progression in many cancers, such as hepatocellular carcinoma[12] and prostate cancer[13]. Besides, SNHG7 expedited NB progression

Corresponding Author: Chunyu Zhang, MD; e-mail: zzy0228@Sina.com

by sponging microRNA-653-5p and increasing STAT2 expression[14]. Nevertheless, the role of SNHG7 in cisplatin sensitivity of NB remains unclear.

MicroRNAs (miRNAs) are small RNAs composed of 18-25 nucleotides, lacking protein-coding ability[15]. Accumulating evidence has confirmed that lncRNAs modulate mRNAs expression *via* acting as sponges for miRNAs[16]. SNHG7 also functions as a miRNA sponge in several types of cancers[17]. Of note, SNHG7 sponged miR-324-3p to facilitate the epithelial-mesenchymal transition of prostate cancer by upregulating WNT2B[13]. Yang et al[18] revealed that miR-329 was lowly expressed in NB and curbed the metastasis of NB cells. However, the specific mechanism of miR-329-3p in NB chemoresistance has not been explored.

Myosin X (MYO10) is a motor protein that links to a variety of diseases[19], and it was observably upregulated in metastatic cancers such as breast cancer and non-small-cell lung cancer[20,21]. Wang et al[22] found that miR-129 targeted MYO10 to enhance the chemosensitivity of NB. However, the relationship between MYO10 and miR-329-3p has not been investigated.

Therefore, we examined the expression of SNHG7 in NB tissues and cells. Furtherly, we explored the role of SNHG7 in chemosensitivity and autophagy and its potential mechanisms.

Patients and Methods

Specimen Collection

Twenty-six NB tissues and matched adjacent normal tissues were obtained from patients with NB at The Fifth Affiliated Hospital of Harbin Medical University. None of the patients received preoperative treatment. All participants signed written informed consents. The present research obtained the approval of the Ethics Committee of The Fifth Affiliated Hospital of Harbin Medical University.

Cell Culture

Human umbilical vein endothelial cell line HUVEC and NB cell line SK-N-AS were commercially obtained from American Type Culture Collection (ATCC, Manassas, VA, USA). NB cell line LAN-6 was purchased from BinSuiBio (Shanghai, China). Cells were incubated in Roswell Park Memorial Institute-1640 (RPMI-1640; Solarbio, Shanghai, China) supplemented with 10% fetal bovine serum (FBS; Solarbio) at 37°C with 5% CO_2.

Cell Transfection

Small interfering RNA (siRNA) against SNHG7 (si-SNHG7), siRNA negative control (si-NC), miR-329-3p mimic (miR-329-3p), the mimic control (miR-NC), miR-329-3p inhibitor (anti-miR-329-3p), the inhibitor control (anti-miR-NC), SNHG7 overexpression vector (pcDNA-SNHG7), MYO10 overexpression vector (pcDNA-MYO10) and the empty overexpression vector (pcDNA-NC) were obtained from Ribobio (Guangzhou, China). Lipofectamine 3000 (Invitrogen, Carlsbad, CA, USA) was used to transfect oligonucleotides and plasmids into NB cells.

Quantitative Real Time-Polymerase Chain Reaction (qRT-PCR)

RNA extraction was carried out using TRIzol reagent (Invitrogen, Carlsbad, CA, USA). The first-strand of complementary DNA (cDNA) was synthesized using M-MLV RT Kit (AiYou Biosciences, Guangzhou, China) or miScript II RT Kit (Qiagen, Hilden, Germany). SYBR Green PCR Master Mix (LMAI Bio, Shanghai, China) was used to perform quantitative RT-PCR. Glyceraldehyde-3-phosphate dehydrogenase (GAPDH) or U6 small RNA was used as the internal control. The primers were as follows: SNHG7-F: 5'-CGATCGATATGCTAGCTAGC-3', SNHG7-R, 5'-CGTAGCTAGCGTAGCGTAT-3'; miR-329-3p-F: 5'-GGGAACACACCTGGTTAAC-3', miR-329-3p-R, 5'-CAGTGCGTGTCGTGGAGT-3'; MYO10-F: 5'-GAACCCCTACCAGCCCATC-3', MYO10-R, 5'-GTTTTACCTGCCCCACTTTCA-3'; GAPDH-F: 5'-ACAACTTTGGTATCGTGGAAGG-3', GAPDH-R, 5'-GCCATCACGCCACAGTTTC-3'; U6-F: 5'-CTCGCTTCGGCAGCACA-3', U6-R, 5'-ACGCTTCACGAATTTGCGT-3'.

Cell Counting Kit-8 (CCK-8) Assay

NB cells were plated into 96-well plates and then treated with different doses of cisplatin (0 μM, 5 μM, 10 μM, 15 μM, 20 μM, 25 μM, 30 μM, 35 μM and 40 μM) for 24 h. Next, 10 μL CCK-8 solution (Beyotime, Shanghai, China) was added into each well and incubated for 2 h. The absorbance was examined at 450 nm using a microplate reader (Thermo Fisher Scientific, Waltham, MA, USA). The half inhibition concentration (IC_{50}) of cisplatin was calculated using the cell viability curve.

Western Blot Assay

In brief, cells were lysed with radioimmunoprecipitation assay (RIPA) buffer (Beyotime, Shanghai, China). Equal amounts of protein were separated by sodium dodecyl sulfate polyacrylamide gel electrophoresis (SDS-PAGE) and transferred to polyvinylidene difluoride (PVDF) membranes (Millipore, Billerica, MA, USA). After blocking with 5% skim milk for 2 h, the membranes were incubated with primary antibodies against LC3B (ab48394, Abcam, Cambridge, UK), Beclin-1 (ab62557, Abcam, Cambridge, UK), p62 (ab109012, Abcam, Cambridge, UK), MYO10 (ab58699, Abcam, Cambridge, UK) or GAPDH (ab9485, Abcam, Cambridge, UK) at a dilution ratio of 1:1000. Later, the membranes were interacted with secondary antibody (ab7090, Abcam, Cambridge, UK). The signal intensity was measured by the enhanced chemiluminescence (ECL) system (Millipore, Billerica, MA, USA).

Dual-Luciferase Reporter Assay

SK-N-AS and LAN-6 cells were plated in 24-well plates. The sequences of SNHG7 or MYO10 3'UTR containing wild-type or mutant binding sites of miR-329-3p were inserted into the pmirGLO vector (Promega, Madison, WI, USA). The corresponding Luciferase reporter and miR-329-3p mimic or miR-NC were cotransfected into NB cells. Finally, the Luciferase activity was examined by Dual-Luciferase Assay Kit (Solarbio).

Statistical Analysis

GraphPad Prism 7.0 software (GraphPad Inc., La Jolla, CA, USA) was executed to analyze data. Data were expressed as mean ± standard deviation of three independent experiments. Differences were compared using Student's *t*-test or one-way analysis of variance (ANOVA). Spearman's correlation analysis was utilized to assess the correlation among SNHG7, miR-329-3p and MYO10. $p<0.05$ was considered statistically significant.

Results

Cisplatin Hindered Cell Viability and Induced Autophagy In NB Cells

To explore the effect of cisplatin on cell viability, SK-N-AS and LAN-6 cells were incubated with different doses of cisplatin (0 μM, 5 μM, 10 μM, 15 μM, 20 μM, 25 μM, 30 μM, 35 μM and 40 μM) for 24 h. CCK-8 assay indicated that cisplatin dramatically reduced the viability of SK-N-AS and LAN-6 cells in a dose-dependent manner (Figure 1A and 1B). The IC_{50} of cisplatin to SK-N-AS and LAN-6 cells were 19.33 μM and 29.67 μM, respectively (Figure 1C). In addition, Western blot analysis was used to determine the expression of autophagy-related proteins in NB cells treated with the corresponding IC_{50} of cisplatin. The results revealed that cisplatin remarkably elevated the ratio of LC3B-II/LC3B-I and Beclin-1 expression and decreased p62 expression compared with the control group (Figure 1D and 1E). These data concluded that cisplatin inhibited cell viability and expedited autophagy in NB cells.

Depletion of SNHG7 Enhanced Cisplatin Sensitivity and Suppressed Cisplatin-Induced Autophagy

To investigate the role of SNHG7 in cisplatin sensitivity, we first measured SNHG7 expression in NB tissues using qRT-PCR. The results exhibited that SNHG7 expression was distinctly increased in NB tissues compared with the normal tissues (Figure 2A). As shown in Figure 2B, SNHG7 expression in SK-N-AS and LAN-6 cells was overtly higher than that in HUVEC cells. Additionally, the expression of SNHG7 in NB cells transfected with si-SNHG7 was notably reduced compared with the si-NC group, indicating significant knockdown efficiency (Figure 2C). Next, increasing concentrations of cisplatin were added to SK-N-AS and LAN-6 cells after transfection for 24 h. CCK-8 assay suggested that knockdown of SNHG7 markedly decreased the IC_{50} of cisplatin in SK-N-AS and LAN-6 cells (Figure 2D-2G). Moreover, transfected SK-N-AS and LAN-6 cells were incubated with cisplatin (19.33 μM and 29.67 μM, respectively) for 24 h. Western blot analysis showed that SNHG7 knockdown and cisplatin treatment resulted in a distinct decrease in LC3B-II/LC3B-I ratio and Beclin-1 expression and a notable increase in p62 expression compared to cisplatin treatment alone (Figure 2H and 2I). These data indicated that SNHG7 silencing potentiated cisplatin sensitivity and inhibited cisplatin-induced autophagy.

SNHG7 Was a Sponge of MiR-329-3p

First, the online database StarBase3.0 predicted that SNHG7 and miR-329-3p had putative binding sites (Figure 3A). Next, Dual-Luciferase reporter assay was utilized to confirm whether SNHG7 targeted miR-329-3p, and the results

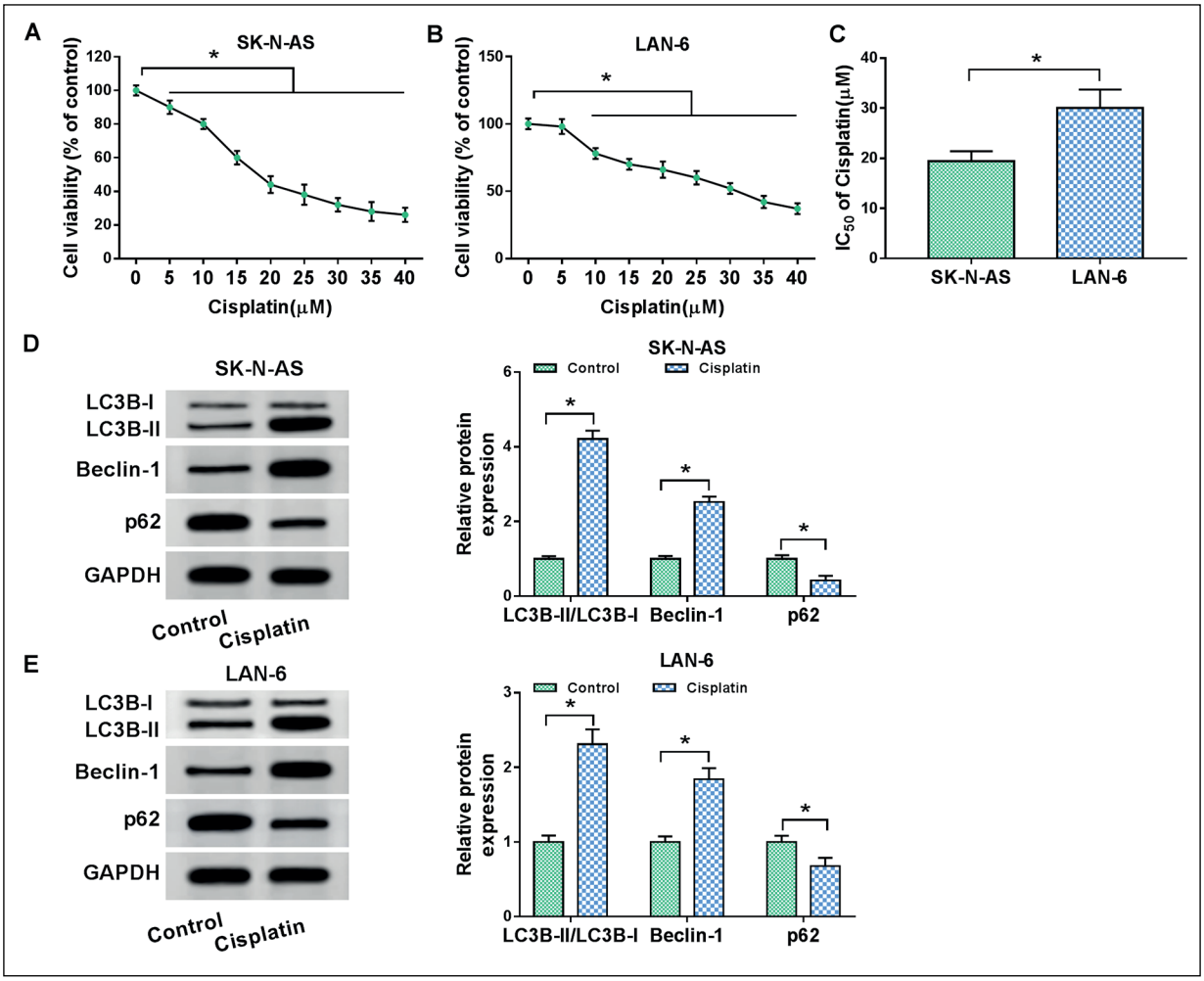

Figure 1. Cisplatin hindered cell viability and induced autophagy in NB cells. **A-C**, SK-N-AS and LAN-6 cells were incubated with different concentrations of cisplatin (0 μM, 5 μM, 10 μM, 15 μM, 20 μM, 25 μM, 30 μM, 35 μM and 40 μM) for 24 h. CCK-8 assay was conducted to evaluate cell viability and IC_{50} value after cisplatin treatment. **D, E,** The expression of autophagy-related proteins in SK-N-AS and LAN-6 cells incubated with 19.33 μM or 29.67 μM cisplatin was detected using western blot assay. *$p < 0.05$.

discovered that miR-329-3p mimic strikingly reduced the Luciferase activity of SNHG7-WT reporter in SK-N-AS and LAN-6 cells (Figure 3B and 3C). Moreover, SNHG7 depletion observably increased the expression of miR-329-3p, while the increase was abrogated after transfection with anti-miR-329-3p (Figure 3D and 3E). SNHG7 overexpression remarkably reduced the level of miR-329-3p, whereas the level was abated by upregulating miR-329-3p (Figure 3F and 3G). In addition, miR-329-3p expression was overtly decreased in NB tissues and cells (Figure 3H and 3I). Spearman's correlation analysis found that SNHG7 expression was negatively correlated with miR-329-3p expression in NB tissues (Figure 3J). These data evidenced that SNHG7 negatively targeted miR-329-3p in NB cells.

SNHG7 Regulated Cisplatin Sensitivity and Cisplatin-Induced Autophagy by Sponging MiR-329-3p

Restoration experiments were performed to elucidate the function of SNHG7 targeting miR-329-3p in cisplatin sensitivity. First of all, the viability of NB cells and IC_{50} of cisplatin were predominantly reduced after transfection with si-SNHG7 compared with the si-NC group, while cotransfection with si-SNHG7 and anti-miR-329-3p reversed the effect (Figure 4A-4D). Besides, introduced with si-SNHG7 and treated with cisplatin led to a significant reduction in LC3B-II/LC3B-I ratio and Be-

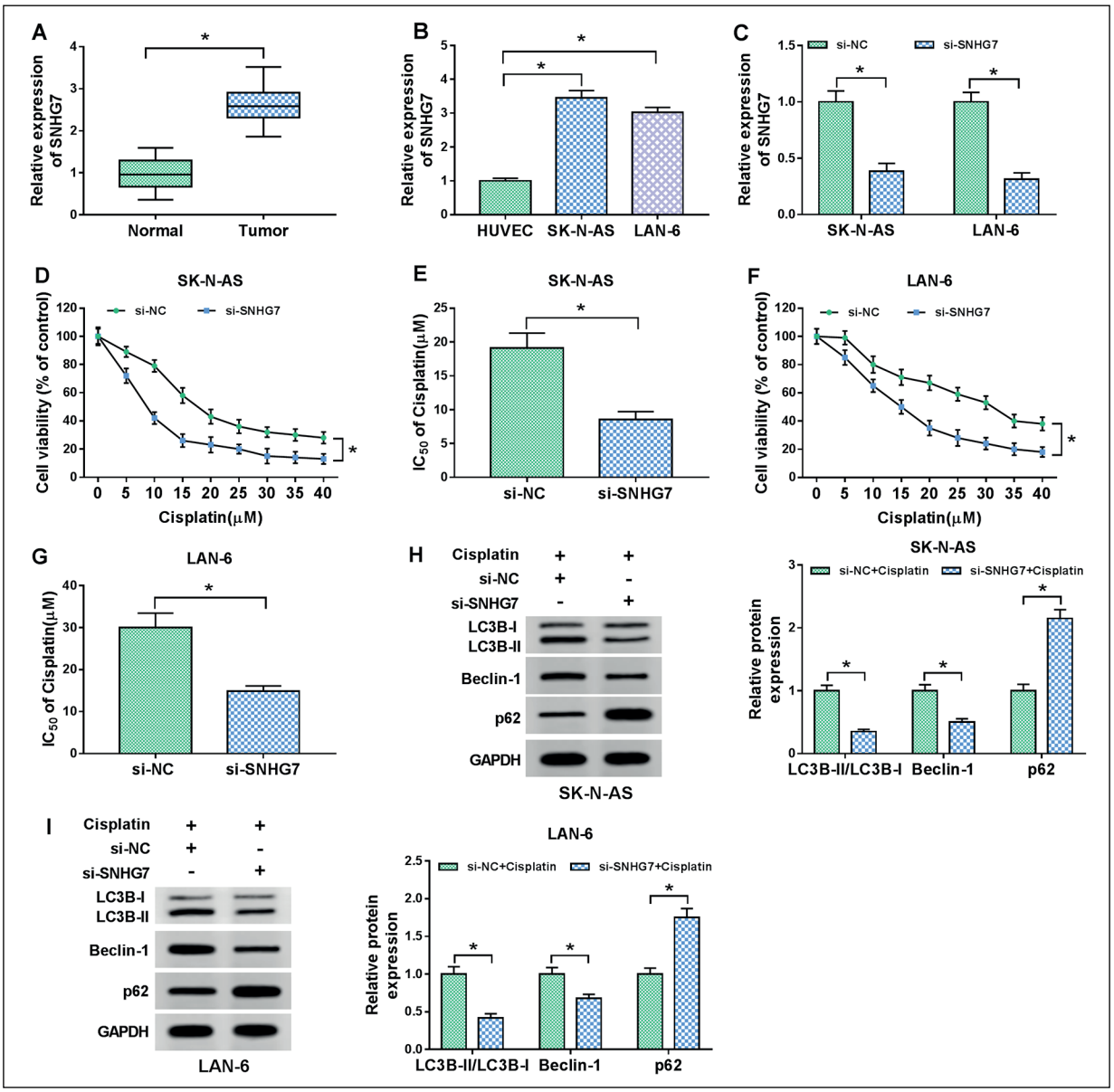

Figure 2. Depletion of SNHG7 enhanced cisplatin sensitivity and suppressed cisplatin-induced autophagy. **A**, The expression of SNHG7 in 26 NB tissues and matched non-tumor tissues was detected by qRT-PCR. **B**, SNHG7 expression was measured in human umbilical vein endothelial cells HUVEC and NB cell lines. **C-I**, SK-N-AS and LAN-6 cells were introduced with si-NC or si-SNHG7. **C**, SNHG7 level was tested by qRT-PCR. **D, E**, Cell viability and IC_{50} value of SK-N-AS cells were determined by CCK-8 assay after treatment with different doses of cisplatin. **F, G**, Cell viability and IC_{50} value of LAN-6 cells were evaluated by CCK-8 assay after incubation with cisplatin (0-40 μM). **H, I**, Transfected SK-N-AS and LAN-6 cells were treated with cisplatin (19.33 μM and 29.67 μM, respectively), and then the protein levels of autophagy markers were measured by western blot assay. *$p < 0.05$.

clin-1 expression and an evident increase in p62 expression compared with the si-NC+cisplatin group, whereas the effect was reverted by the inhibition of miR-329-3p (Figure 4E and 4F). These data manifested that knockdown of SNHG7 reduced cisplatin resistance and impeded cisplatin-induced autophagy in NB cells *via* regulating miR-329-3p.

SNHG7 Sponged MiR-329-3p to Regulate MYO10 Expression

To further explore the potential mechanism of SNHG7, the online database StarBase3.0 was used to predict miR-329-3p targets. As displayed in Figure 5A, miR-329-3p and MYO10 3'UTR had putative complementary sequences. Next, Du-

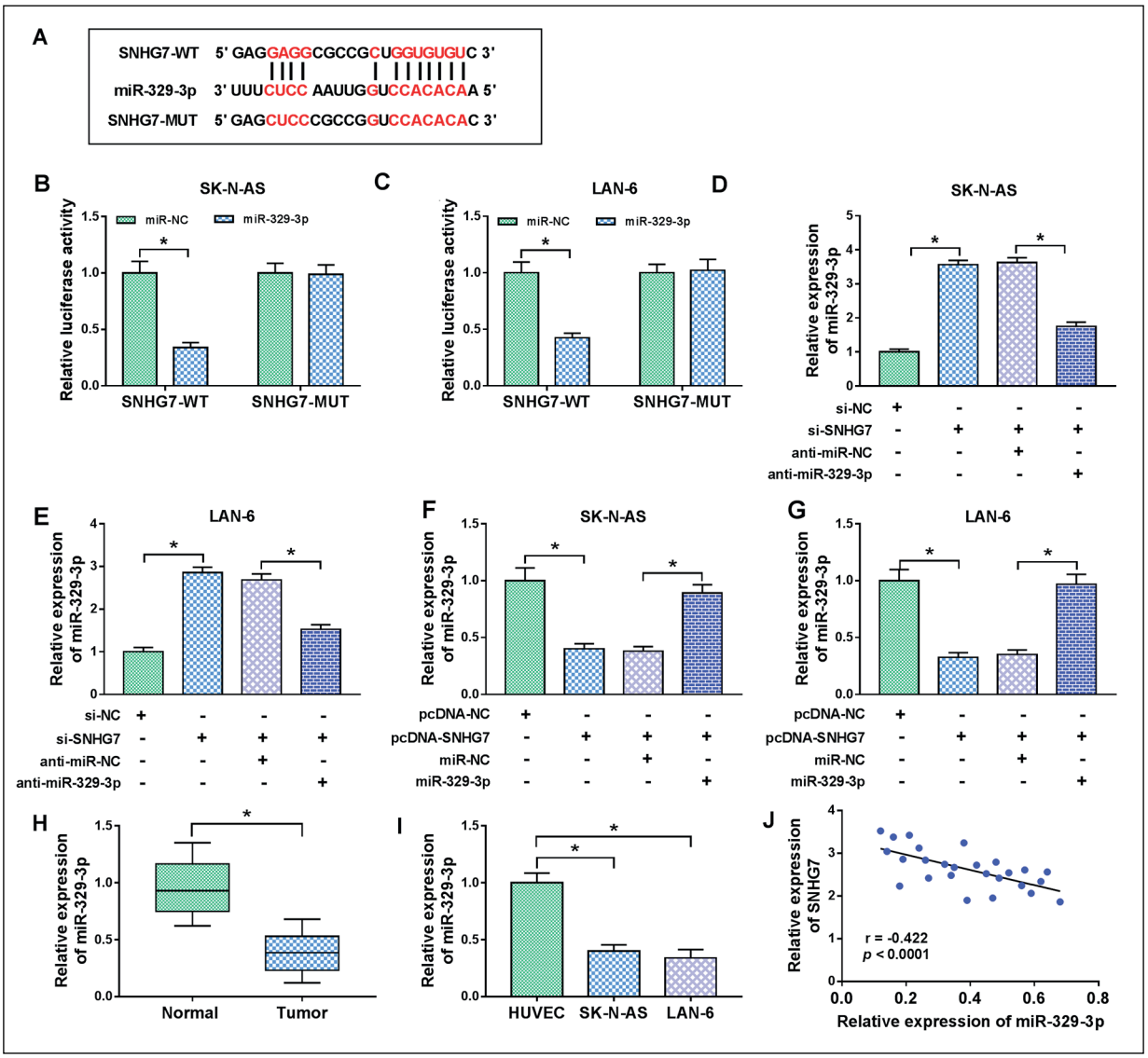

Figure 3. SNHG7 was a sponge of miR-329-3p. **A**, The predicted binding sites of SNHG7 and miR-329-3p were exhibited. **B, C,** Dual-luciferase reporter assay was utilized to validate the relationship between SNHG7 and miR-329-3p. **D, E,** The expression of miR-329-3p was examined in SK-N-AS and LAN-6 cells introduced with si-NC, si-SNHG7, si-SNHG7+anti-miR-NC or si-SNHG7+anti-miR-329-3p. **F, G,** The level of miR-329-3p was measured in SK-N-AS and LAN-6 cells transfected with pcDNA-NC, pcDNA-SNHG7, pcDNA-SNHG7+ miR-NC or pcDNA-SNHG7+miR-329-3p. **H**, The expression of miR-329-3p was detected in NB tissues and matched non-tumor tissues. **I**, MiR-329-3p expression was tested in HUVEC cells and NB cell lines. **J**, The correlation between SNHG7 and miR-329-3p levels in NB tissues was analyzed by Spearman's correlation analysis. *$p < 0.05$.

al-Luciferase reporter assay disclosed that miR-329-3p mimic drastically decreased the Luciferase activity of MYO10 3'UTR-WT reporter, but the Luciferase activity was not affected when the binding sites were mutated (Figure 5B and 5C). In addition, the mRNA and protein expression of MYO10 were prominently elevated in NB tissues relative to the normal tissues (Figure 5D and 5E). Compared with HUVEC cells, the mRNA and protein expression of MYO10 was markedly increased in NB cells (Figure 5F and 5G). In NB tissues, MYO10 and miR-329-3p levels were negatively correlated, while MYO10 and SNHG7 levels were positively correlated (Figure 5H and 5I). Moreover, the results of qRT-PCR and Western blot indicated that transfection with miR-329-3p resulted in an apparent decrease in the mRNA and protein expression of MYO10, while the effect was

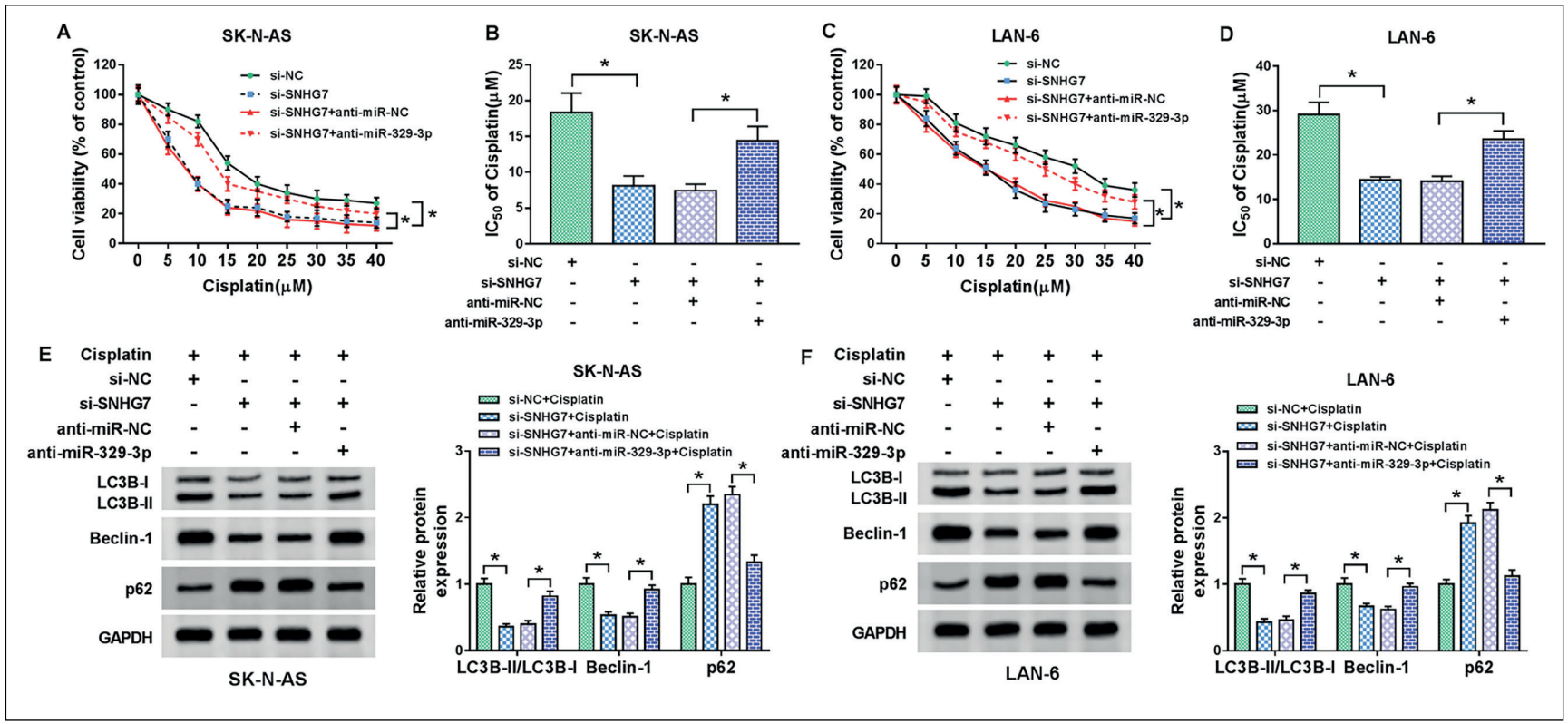

Figure 4. SNHG7 regulated cisplatin sensitivity and cisplatin-induced autophagy by sponging miR-329-3p. SK-N-AS and LAN-6 cells were introduced with si-NC, si-SNHG7, si-SNHG7+anti-miR-NC or si-SNHG7+anti-miR-329-3p. **A-D**, Transfected SK-N-AS and LAN-6 cells were cultured with different concentrations of cisplatin for 24 h, and CCK-8 assay was performed to evaluate cell viability and the IC_{50} of cisplatin. **E, F**, After treated with cisplatin (19.33 μM and 29.67 μM, respectively), the protein levels of autophagy markers in SK-N-AS and LAN-6 cells were measured by Western blot assay. *$p < 0.05$.

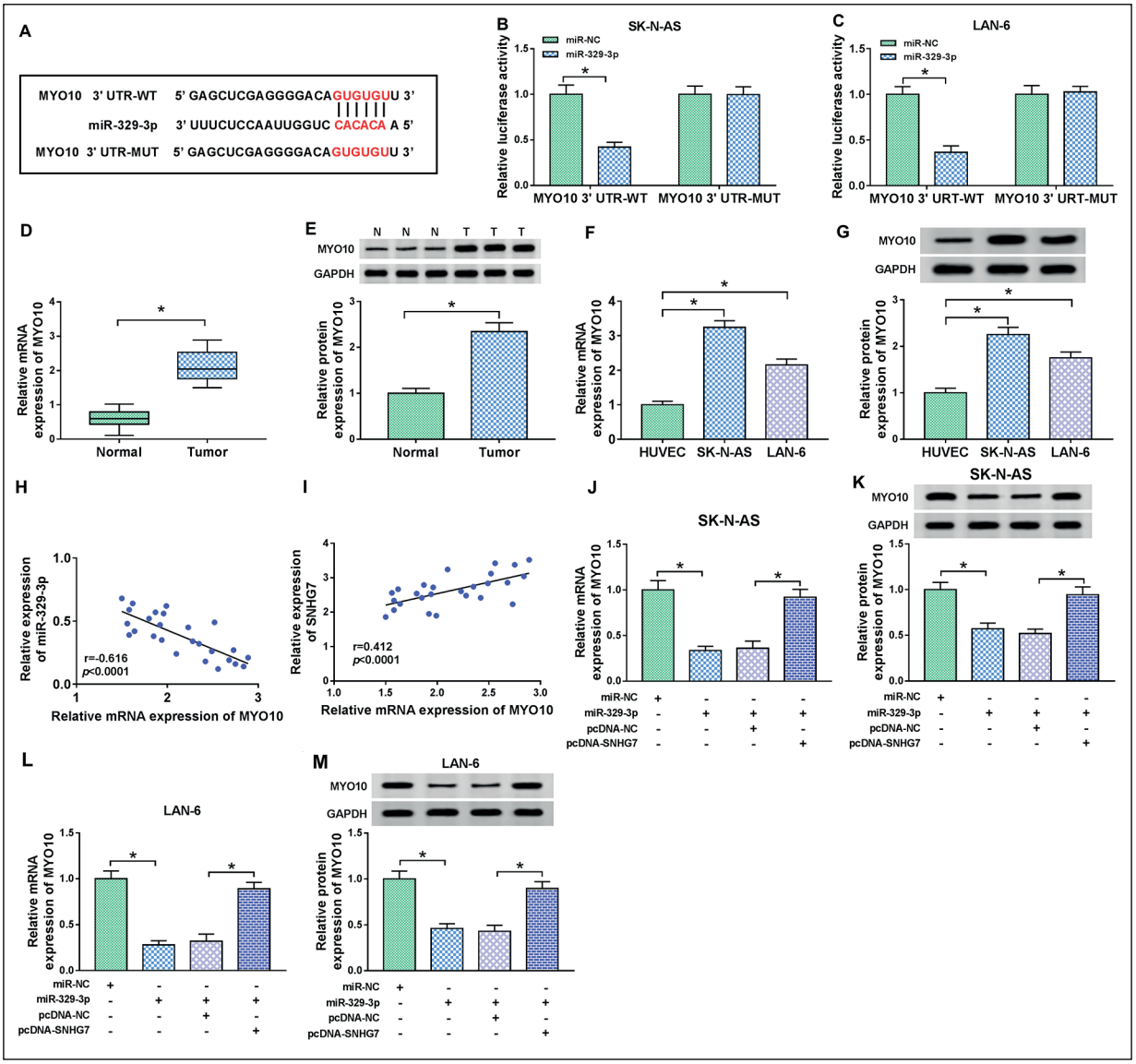

Figure 5. SNHG7 sponged miR-329-3p to regulate MYO10 expression. **A,** The putative binding sites of miR-329-3p and MYO10 3'UTR were displayed. **B, C,** Dual-luciferase reporter assay was conducted to confirm the relationship between miR-329-3p and MYO10. **D, E,** The mRNA and protein levels of MYO10 were detected in NB tissues and matched non-tumor tissues using qRT-PCR and Western blot. **F, G,** The mRNA and protein levels of MYO10 were examined in HUVEC cells and NB cell lines. **H, I,** The interaction among SNHG7, miR-329-3p and MYO10 was assessed by Spearman's correlation analysis. **J-M,** The mRNA and protein levels of MYO10 were measured in SK-N-AS and LAN-6 cells introduced with miR-NC, miR-329-3p, miR-329-3p+pcDNA-NC or miR-329-3p+pcDNA-SNHG7. *$p < 0.05$.

undermined after cotransfection with miR-329-3p and pcDNA-SNHG7 (Figure 5J-5M). These data discovered that SNHG7 sponged miR-329-3p to regulate MYO10 expression in NB cells.

MiR-329-3p Modulated Cisplatin Sensitivity and Cisplatin-Induced Autophagy by Targeting MYO10

To investigate whether miR-329-3p regulated cisplatin sensitivity *via* targeting MYO10, SK-N-AS and LAN-6 cells were introduced with miR-NC, miR-329-3p, miR-329-3p+pcDNA-NC or miR-329-3p+pcDNA-MYO10. First, the expression of MYO10 was determined by qRT-PCR and Western blot. The results showed that MYO10 overexpression abrogated the inhibitory effect of miR-329-3p mimic on the mRNA and protein levels of MYO10 (Figure 6A-6D). Furthermore, upregulation of miR-329-3p restrained the viability of NB cells and IC_{50} of cisplatin, while the effect

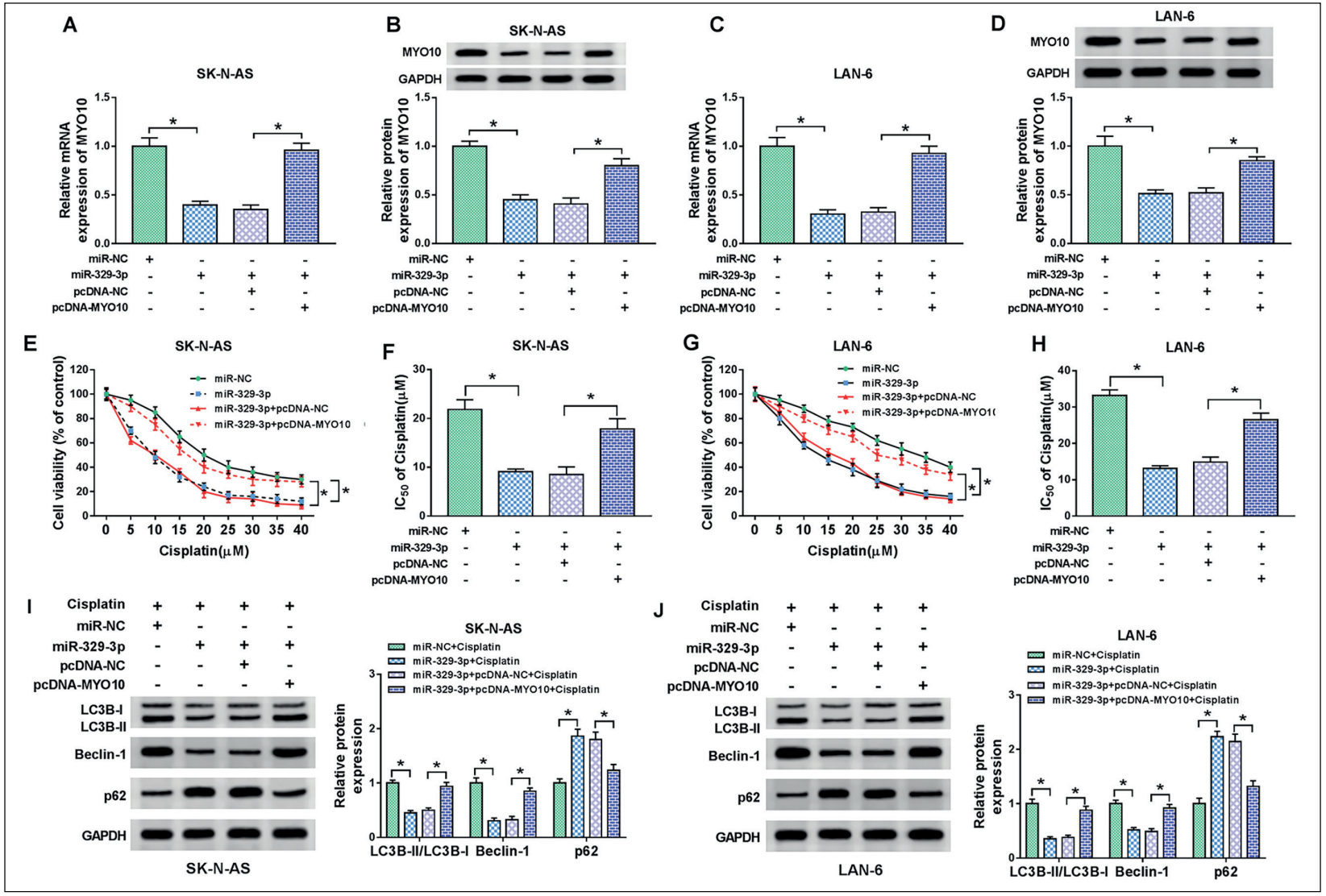

Figure 6. MiR-329-3p modulated cisplatin sensitivity and cisplatin-induced autophagy by targeting MYO10. SK-N-AS and LAN-6 cells were transfected with miR-NC, miR-329-3p, miR-329-3p+pcDNA-NC or miR-329-3p+pcDNA-MYO10. **A-D**, The mRNA and protein levels of MYO10 were detected in transfected SK-N-AS and LAN-6 cells. **E-H,** After cell transfection, NB cells were incubated with different concentrations of cisplatin for 24 h, and then CCK-8 assay was used to evaluate cell viability and the IC_{50} of cisplatin. **I, J,** After transfection for 24 h, SK-N-AS and LAN-6 cells were treated with 19.33 μM and 29.67 μM cisplatin, respectively, and autophagy-related protein levels were detected by Western blot analysis. *$p < 0.05$.

was abolished by increasing MYO10 expression (Figure 6E-6H). Western blot analysis revealed a remarkable reduction in LC3B-II/LC3B-I ratio and Beclin-1 expression and a marked increase in p62 expression in the miR-329-3p+cisplatin group compared to the miR-NC+cisplatin group, but these results were reversed after transfection with pcDNA-MYO10 (Figure 6I and 6J). These data corroborated that miR-329-3p could increase cisplatin sensitivity and suppress cisplatin-induced autophagy in NB cells by targeting MYO10.

Inhibition of Autophagy Impeded SNHG7-Induced Cisplatin Resistance

To explore the role of autophagy in SNHG7-induced cisplatin resistance, SK-N-AS and LAN-6 cells were treated with or without 3-MA (5 MM). CCK-8 assay suggested that 3-MA treatment had no significant effect on the viability of NB cells (Figure 7A). SNHG7 upregulation resulted in a notable increase in LC3B-II/LC3B-I ratio and Beclin-1 expression and a significant reduction in p62 expression, while the levels were reversed after treatment with 3-MA (Figure 7B and 7C). Moreover, SNHG7 overexpression increased the IC_{50} of cisplatin, whereas transfection with pcDNA-SNHG7 and treatment with 3-MA recuperated the effect (Figure 7D and 7E). All these results indicated that inhibition of autophagy hindered cisplatin resistance in NS cells induced by SNHG7.

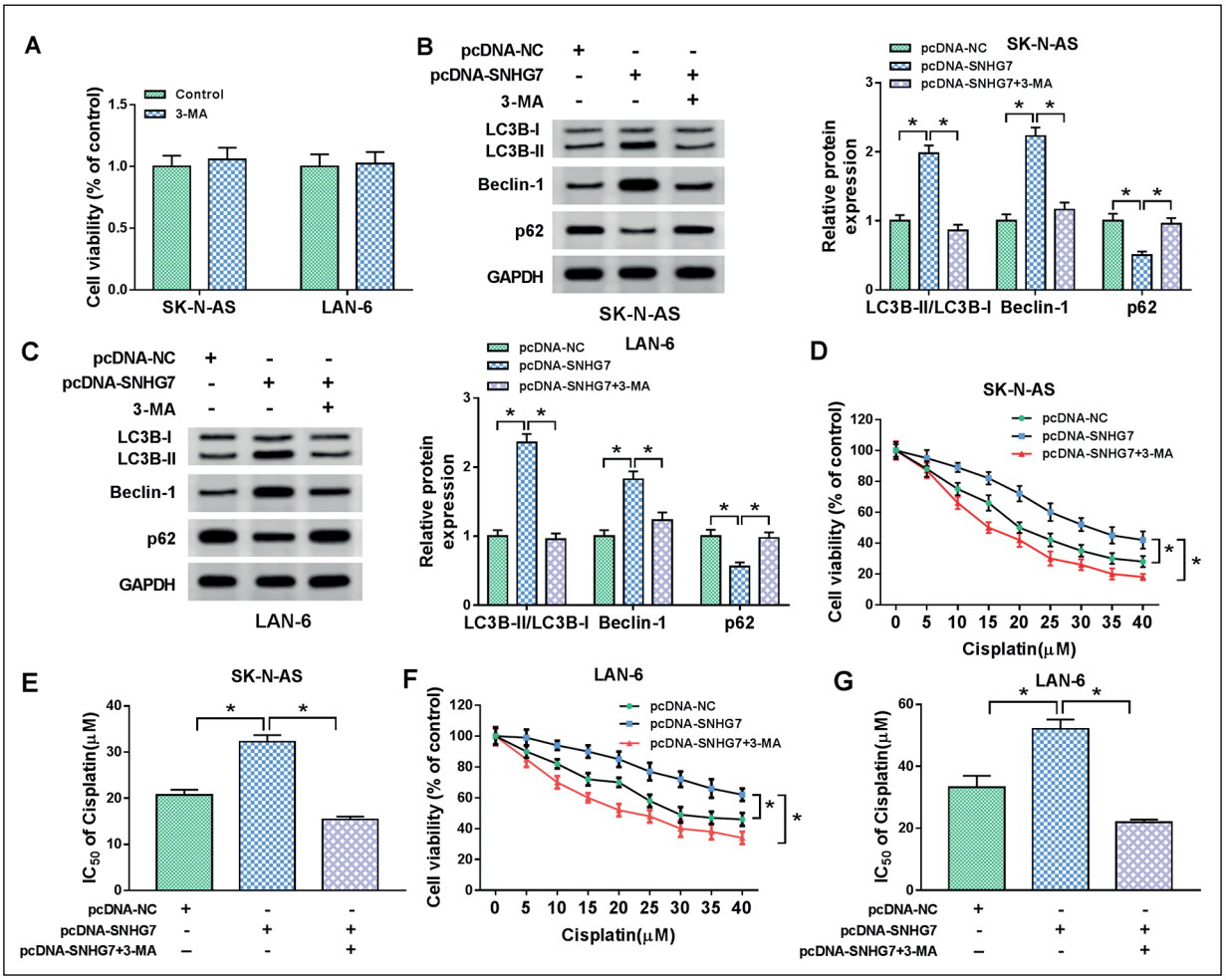

Figure 7. Inhibition of autophagy impeded SNHG7-induced cisplatin resistance. **A,** SK-N-AS and LAN-6 cells were treated with 3-MA (5 MM), and cell viability was detected using CCK-8 assay. **B-G,** SK-N-AS and LAN-6 cells were transfected with pcDNA-NC or pcDNA-SNHG7, and cells partially transfected with pcDNA-SNHG7 were incubated with 3-MA (5 MM). **B, C,** The autophagy-related protein levels were measured by Western blot analysis. **D-G,** CCK-8 assay was used to assess cell viability and calculate the IC_{50} of cisplatin. *$p < 0.05$.

Discussion

Chemotherapy resistance is a major stumbling block in cancer treatment[23]. Autophagy is a crucial regulator of tumor microenvironment and cellular drug response in many types of cancer[24]. During autophagy, LC3B was transformed from the cytosolic LC3B-I form to the lipidated LC3B-II form, and LC3B-II/LC3B-I ratio could be used as an indicator of autophagosome formation[25]. The expression of p62 and Beclin-1 indicated autophagy degradation and accumulation, respectively[26,27]. Besides, aberrant expression of autophagy genes may regulate apoptosis[28]. Deficiency of the Beclin-1 gene results in impaired autophagic flux, usually accompanied by apoptosis[29]. Further research on the mechanisms of chemoresistance and autophagy in NB is important for improving drug sensitivity.

LncRNAs play essential roles in the progression of NB. LncRNA KCNQ1OT1 accelerated cell apoptosis in NB via acting as a sponge for miR-296-5p and elevating Bax expression[30]. Yu et al[31] found that SNHG16 facilitated NB progression and highly expressed SNHG16 was positively correlated with poor clinical outcomes. Ye et al[32] disclosed that linc01105 contributed to NB development, which acted by sponging miR-6769b-5p and upregulating VEGFA. In addition, SNHG7 was strikingly upregulated in NB tissues and induced NB progression[14]. Silencing of SNHG7 potentiated cisplatin sensitivity and induced cell apoptosis in non-small cell lung cancer through activation of PI3K/AKT pathway[33]. However, previous reports did not address the effect of SNHG7 on drug sensitivity in NB. In our research, SNHG7 expression was overtly increased in NB tissues and cells. Further, inhibition of SNHG7 declined cisplatin resistance and blocked cisplatin-induced autophagy.

In the present study, we unveiled that miR-329-3p was a target of SNHG7. Intriguingly, previous reports indicated that miR-329 acted as a vital regulator in many types of malignancies. In papillary thyroid cancer, miR-329 functioned as a tumor-suppressing factor by degrading the target gene WNT1[34]. In osteosarcoma, miR-329 impeded tumor development *via* repressing Rab10 expression[35]. Xu et al[36] indicated that miR-329-3p reversed the stimulatory effect of TP73-AS1 on cervical cancer progression. Also, miR-329-3p hindered cell proliferation and metastasis *via* targeting MAPK1[37]. In terms of resistance, miR-329 increased 5-FU sensitivity in colorectal cancer through degradation of E2F1[38]. Nevertheless, the function of miR-329-3p in cisplatin resistance has not been reported. In the current study, SNHG7 strengthened cisplatin resistance and boosted cisplatin-induced autophagy in NB cells *via* sponging miR-329-3p.

MYO10 links integrins and microtubules to stimulate the formation of filopodia[39]. A growing body of evidence has demonstrated that miRNAs bound to the 3'UTR of the target genes, thereby repressing their expression to regulate cell progression[40]. In this research, we observed that miR-329-3p targeted MYO10. Interestingly, MYO10 was identified as a promoting factor of cell transfer[41]. Chen et al[42] presented that miR-340 curbed the metastasis of breast cancer cells by binding to MYO10. In NB, the miR-129/MYO10 axis modulated tumor progression and chemoresistance[22]. The findings of the present study were consistent with previous investigations. MYO10 was prominently upregulated in NB tissues and cells. What's more, miR-329-3p targeted MYO10 to regulate chemosensitivity and cisplatin-induced autophagy in NB cells.

Conclusions

In brief, we demonstrated that inhibition of SNHG7 potentiated cisplatin sensitivity and suppressed autophagy in NB by modulating the miR-329-3p/MYO10 axis. These findings deepened our understanding of NB and provided a new avenue for improving chemoresistance.

Conflict of Interest

The Authors declare that they have no conflict of interests.

References

1) Cheung NK, Dyer MA. Neuroblastoma: developmental biology, cancer genomics and immunotherapy. Nat Rev Cancer 2013; 13: 397-411.
2) Matthay KK. Neuroblastoma: a clinical challenge and biologic puzzle. CA Cancer J Clin 1995; 45: 179-192.
3) Pinto NR, Applebaum MA, Volchenboum SL, Matthay KK, London WB, Ambros PF, Nakagawara A, Berthold F, Schleiermacher G, Park JR, Valteau-Couanet D, Pearson AD, Cohn SL. Advances in risk classification and treatment strategies for neuroblastoma. J Clin Oncol 2015; 33: 3008-3017.
4) Cheung NV, Heller G. Chemotherapy dose intensity correlates strongly with response, median

survival, and median progression-free survival in metastatic neuroblastoma. J Clin Oncol 1991; 9: 1050-1058.

5) Benard J. Genetic alterations associated with metastatic dissemination and chemoresistance in neuroblastoma. Eur J Cancer 1995; 31A: 560-564.

6) Hurley JH, Young LN. Mechanisms of autophagy initiation. Annu Rev Biochem 2017; 86: 225-244.

7) Kaur J, Debnath J. Autophagy at the crossroads of catabolism and anabolism. Nat Rev Mol Cell Biol 2015; 16: 461-472.

8) Levine B, Kroemer G. Biological functions of autophagy genes: a disease perspective. Cell 2019; 176: 11-42.

9) Gao J, Wang W. Knockdown of galectin-1 facilitated cisplatin sensitivity by inhibiting autophagy in neuroblastoma cells. Chem Biol Interact 2019; 297: 50-56.

10) Chandra A, Rick J, Yagnik G, Aghi MK. Autophagy as a mechanism for anti-angiogenic therapy resistance. Semin Cancer Biol 2019 Aug 28. pii: S1044-579X(19)30014-8. doi: 10.1016/j.semcancer.2019.08.031. [Epub ahead of print]

11) Gibb EA, Brown CJ, Lam WL. The functional role of long non-coding RNA in human carcinomas. Mol Cancer 2011; 10: 38.

12) Yang X, Sun L, Wang L, Yao B, Mo H, Yang W. LncRNA SNHG7 accelerates the proliferation, migration and invasion of hepatocellular carcinoma cells via regulating miR-122-5p and RPL4. Biomed Pharmacother 2019; 118: 109386.

13) Han Y, Hu H, Zhou J. Knockdown of LncRNA SNHG7 inhibited epithelial-mesenchymal transition in prostate cancer though miR-324-3p/WNT2B axis in vitro. Pathol Res Pract 2019; 215: 152537.

14) Chi R, Chen X, Liu M, Zhang H, Li F, Fan X, Wang W, Lu H. Role of SNHG7-miR-653-5p-STAT2 feedback loop in regulating neuroblastoma progression. J Cell Physiol 2019; 234: 13403-13412.

15) Yao Q, Chen Y, Zhou X. The roles of microRNAs in epigenetic regulation. Curr Opin Chem Biol 2019; 51: 11-17.

16) Klinge CM. Non-coding RNAs: long non-coding RNAs and microRNAs in endocrine-related cancers. Endocr Relat Cancer 2018; 25: R259-R282.

17) Cheng D, Fan J, Ma Y, Zhou Y, Qin K, Shi M, Yang J. LncRNA SNHG7 promotes pancreatic cancer proliferation through ID4 by sponging miR-342-3p. Cell Biosci 2019; 9: 28.

18) Yang H, Li Q, Zhao W, Yuan D, Zhao H, Zhou Y. MiR-329 suppresses the growth and motility of neuroblastoma by targeting KDM1A. FEBS Lett 2014; 588: 192-197.

19) Courson DS, Cheney RE. Myosin-X and disease. Exp Cell Res 2015; 334: 10-15.

20) Cao R, Chen J, Zhang X, Zhai Y, Qing X, Xing W, Zhang L, Malik YS, Yu H, Zhu X. Elevated expression of myosin X in tumours contributes to breast cancer aggressiveness and metastasis. Br J Cancer 2014; 111: 539-550.

21) Sun Y, Ai X, Shen S, Lu S. NF-kappaB-mediated miR-124 suppresses metastasis of non-small-cell lung cancer by targeting MYO10. Oncotarget 2015; 6: 8244-8254.

22) Wang X, Li J, Xu X, Zheng J, Li Q. MiR-129 inhibits tumor growth and potentiates chemosensitivity of neuroblastoma by targeting MYO10. Biomed Pharmacother 2018; 103: 1312-1318.

23) Rottenberg S, Jonkers J. Modeling therapy resistance in genetically engineered mouse cancer models. Drug Resist Updat 2008; 11: 51-60.

24) Li X, Zhou Y, Li Y, Yang L, Ma Y, Peng X, Yang S, Liu J, Li H. Autophagy: a novel mechanism of chemoresistance in cancers. Biomed Pharmacother 2019; 119: 109415.

25) Huang S, Sinicrope FA. Celecoxib-induced apoptosis is enhanced by ABT-737 and by inhibition of autophagy in human colorectal cancer cells. Autophagy 2010; 6: 256-269.

26) Moscat J, Diaz-Meco MT. p62: a versatile multitasker takes on cancer. Trends Biochem Sci 2012; 37: 230-236.

27) Salminen A, Kaarniranta K, Kauppinen A, Ojala J, Haapasalo A, Soininen H, Hiltunen M. Impaired autophagy and APP processing in Alzheimer's disease: the potential role of Beclin 1 interactome. Prog Neurobiol 2013; 106-107: 33-54.

28) Mulcahy Levy JM, Thorburn A. Autophagy in cancer: moving from understanding mechanism to improving therapy responses in patients. Cell Death Differ 2020; 27: 843-857.

29) Dong G, Zhang Z, Duan K, Shi W, Huang R, Wang B, Luo L, Zhang Y, Ruan H, Huang H. Beclin 1 deficiency causes hepatic cell apoptosis via endoplasmic reticulum stress in zebrafish larvae. FEBS Lett 2019 Dec 10. doi: 10.1002/1873-3468.13712. [Epub ahead of print]

30) Li MM, Liu XH, Zhao YC, Ma XY, Zhou YC, Zhao YX, Liu XY. Long noncoding RNA KCNQ1OT1 promotes apoptosis in neuroblastoma cells by regulating miR-296-5p/Bax axis. FEBS J 2020; 287: 561-577.

31) Yu Y, Chen F, Yang Y, Jin Y, Shi J, Han S, Chu P, Lu J, Tai J, Wang S, Yang W, Wang H, Guo Y, Ni X. lncRNA SNHG16 is associated with proliferation and poor prognosis of pediatric neuroblastoma. Int J Oncol 2019; 55: 93-102.

32) Ye M, Ma J, Liu B, Liu X, Ma D, Dong K. Linc01105 acts as an oncogene in the development of neuroblastoma. Oncol Rep 2019 Aug 2. doi: 10.3892/or.2019.7257. [Epub ahead of print]

33) Chen K, Abuduwufuer A, Zhang H, Luo L, Suotesiyali M, Zou Y. SNHG7 mediates cisplatin-resistance in non-small cell lung cancer by activating PI3K/AKT pathway. Eur Rev Med Pharmacol Sci 2019; 23: 6935-6943.

34) Wu L, Pei F, Men X, Wang K, Ma D. MiR-329 inhibits papillary thyroid cancer progression via direct targeting WNT1. Oncol Lett 2018; 16: 3561-3568.

35) Jiang W, Liu J, Xu T, Yu X. MiR-329 suppresses osteosarcoma development by downregulating Rab10. FEBS Lett 2016; 590: 2973-2981.

36) Xu J, Zhang J. LncRNA TP73-AS1 is a novel regulator in cervical cancer via miR-329-3p/ARF1 axis. J Cell Biochem 2020; 121: 344-352.

37) Li W, Liang J, Zhang Z, Lou H, Zhao L, Xu Y, Ou R. MicroRNA-329-3p targets MAPK1 to suppress cell proliferation, migration and invasion in cervical cancer. Oncol Rep 2017; 37: 2743-2750.

38) Yin J, Shen X, Li M, Ni F, Xu L, Lu H. MiR-329 regulates the sensitivity of 5-FU in chemotherapy of colorectal cancer by targeting E2F1. Oncol Lett 2018; 16: 3587-3592.

39) Sousa AD, Cheney RE. Myosin-X: a molecular motor at the cell's fingertips. Trends Cell Biol 2005; 15: 533-539.

40) Takahashi RU, Prieto-Vila M, Kohama I, Ochiya T. Development of miRNA-based therapeutic approaches for cancer patients. Cancer Sci 2019; 110: 1140-1147.

41) Uhl J, Gujarathi S, Waheed AA, Gordon A, Freed EO, Gousset K. Myosin-X is essential to the intercellular spread of HIV-1 Nef through tunneling nanotubes. J Cell Commun Signal 2019; 13: 209-224.

42) Chen CP, Sun ZL, Lu X, Wu WX, Guo WL, Lu JJ, Han C, Huang JQ, Fang Y. MiR-340 suppresses cell migration and invasion by targeting MYO10 in breast cancer. Oncol Rep 2016; 35: 709-716.